Probing the Exchange Interaction through Micelle Size. 1. Probability of Recombination of Triplet Geminate Radical Pairs

Valery F. Tarasov,[†] Naresh D. Ghatlia,[‡] Anatolii L. Buchachenko,*[,†] and Nicholas J. Turro*[,‡]

Contribution from the Institute of Chemical Physics, 4 Kosygin Street, Moscow 117334, Russia, and Department of Chemistry, Columbia University, New York, New York 10027.
Received June 1, 1992

Abstract: The probability of recombination (P_r) of the primary geminate radical pairs derived from optically active methyldeoxybenzoin (MDB) and from diastereomerically pure 2,4-diphenylpentan-3-one (DPP) have been determined in alkyl sulfate micelles of different sizes. These probabilities have been measured by monitoring the extent of isomerization in the recovered ketone as a function of conversion. The P_r values for these two ketones, as a function of micelle size, display disparate behavior: P_r for MDB increases as the micelle size increases, while P_r for DPP decreases as the micelle size increases. Simple kinetic models which neglect distance-dependent interactions fail, even qualitatively, in predicting this trend. A theoretical treatment which explicitly considers (1) a distance-dependent electron spin exchange interaction (ESE), (2) micelles with a permeable boundary and (3) a coefficient of mutual diffusion that is a function of the micelle size is presented. The permeability of the micelle boundary is treated by introduction of a boundary factor in an improved theoretical model. This adjustment allows us to model radical escape as only occuring from the boundary and does not force us to consider it as a site-independent monoexponential process. Experimental evidence for a micelle size-dependent coefficient of mutual diffusion is presented. Reasonable fits for MDB and DPP, at both the qualitative and quantitative levels, are obtained using this model; omission of any one of the three parameters during the fitting procedure results in an unacceptable deterioration in the quality of the match between the measured and the calculated values. The qualitative result is that there is an increase in the effectiveness of the ESE in suppressing intersystem crossing as the micelle size decreases. For smaller micelles this results in the rate of intersystem crossing becoming the rate-limiting step. The rate of intersystem crossing in these radical pairs is determined not by pure hyperfine interactions but rather by hyperfine interactions modulated by the distance-dependent ESE.

Introduction

Geminate radical reactions conducted under conditions of specially designed geometrical restrictions on the distribution and motion of the radicals are ideal systems for the investigation of the distance-dependent interactions between the radical fragments. Studies of biradicals[1,2] with a variable length tether connecting the two radical centers, radical pairs (RP) solubilized in micelles[2,3] and radicals generated within zeolitic cavities[4] exemplify this approach.

Undoubtedly, biradicals have received the most attention in such efforts. In particular, it was shown that distance-dependent magnetic interactions such as electron spin exchange[1a-e] (ESE) and spin orbit coupling[1f-j] (SOC) do play a major role in determining the reaction rates in these systems. This occurs despite the fact that the strength of these interactions is smaller than k_BT for the distances under consideration. The reason[5] lies in the spin selectivity of radical-radical reactions, the influence of these interactions on the rate of intersystem crossing (ISC), and the fact that the energy required for ISC must be magnetic in character.

The characteristic size of micelles[6] (10-30 Å for alkyl sulfates or quaternary ammonium salts) is comparable in value with the characteristic size of biradicals, defined as the length of the interconnecting chain in the all-trans configuration. Therefore, it was not surprising that the magnetic field dependence of the ^{13}C chemically induced dynamic nuclear polarization (CIDNP) intensity from recombination products of micellized RP qualitatively resembles[3a] that seen for biradicals.[1j,k,7] A key distinction between biradicals and micellized RPs, however, is that the micellized RPs may not be considered as an isolated system during the entire lifetime of the paramagnetic fragments: individual radicals in a RP may exit the micelle into the bulk solvent, whereas the radical centers in a biradical are forced to remain geminate. Other considerations which prevent a more immediate and quantitative comparison between biradicals and micellized RPs include the nonrandom relative motion of the radical centers in biradicals (determined by chain dynamics) as opposed to the completely incoherent motion of the radical centers in RPs relative to one another. Thus, a separate comprehensive investigation of the influence of the micelle size on the chemical behavior of micellized RPs is both germane and needed.

It has been found that the rate of reaction (which is proportional to the cage effect) of geminate radical pairs created by electron

[†] Institute of Chemical Physics.
[‡] Columbia University.

(1) Maeda, K.; Terazima, M.; Azumi, T.; Tanimoto, Y. *J. Phys. Chem.* **1991**, *95*, 197. (b) Staerk, H.; Busman, H.-G.; Kuhnle, W.; Treichel, R. *J. Phys. Chem.* **1991**, *95*, 1906. (c) Busman, H.-G.; Starek, H.; Weller, A. *J. Chem. Phys.* **1989**, *91*, 4098. (d) Tanimoto, Y.; Takashima, M.; Hasegawa, K.; Itoh, M. *Chem. Phys. Lett.* **1987**, *137*, 330. (e) Bittl, R.; Schulten, K. *Chem. Phys. Lett.* **1988**, *146*, 58. (f) Wang, J.-F.; Doubleday, C. H., Jr.; Turro, N. J. *J. Am. Chem. Soc.* **1989**, *111*, 3962. (g) Turro, N. J.; Doubleday, C. H., Jr.; Hwang, K.-C.; Cheng, C.-C.; Fehlner, J. R. *Tetrahedron Lett.* **1987**, *28*, 2929. (h) Zimmt, M. B.; Doubleday, C. H., Jr.; Gould, I. R.; Turro, N. J. *J. Am. Chem. Soc.* **1985**, *107*, 6724. (i) Closs, G. L.; Redwine, O. D. *J. Am. Chem. Soc.* **1985**, *107*, 6131. (j) Closs, G. L.; Miller, R.; Redwine, O. D. *Acc. Chem. Res.* **1985**, *18*, 196. (k) Closs, G. L. In *Chemically Induced Magnetic Polarization*; Muus, L. T., Atkins, P. W. McLauchlan, K. A., Pedersen, J. B., Eds.; Reidel, D.: Dordrecht, Holland, 1977. (l) Levin, P. P.; Kuzmin, V. A. *Bull. Acad. Sci. USSR Div. Chem. Sci.* **1988**, *37*, 224.

(2) Lei, X.-G. *Res. Chem. Intermed.* **1990**, *14*, 15.

(3) (a) Zimmt, M. B.; Doubleday, C. H., Jr.; Turro, N. J. *J. Am. Chem. Soc.* **1984**, *106*, 3363. (b) Closs, G. L.; Forbes, M. D. E.; Norris, J. R., Jr. *J. Phys. Chem.* **1987**, *91*, 3592. (c) Shkrob, I. A.; Tarasov, V. F.; Bagrayanskaya, E. G. *Chem. Phys.* **1991**, *153*, 427. (d) Shkrob, I. A.; Tarasov, V. F.; Buchanchenko, A. L. *Chem. Phys.* **1991**, *153*, 443. (e) Weller, A.; Staerk, H.; Treiche, R. *Faraday Discuss. Chem. Soc.* **1984**, *78*, 271.

(4) (a) Ramamurthy, V.; Caspar, J. V.; Corbin, D. R.; Eaton, D. F.; Kaufman, J. S.; Dybowski, C. *J. Photochem. Photobiol. A: Chem.* **1990**, *51*, 259. (b) Ramamurthy, V.; Corbin, D. R.; Turro, N. J.; Zhang, Z.; Garcia-Garibay, M. A. *J. Org. Chem.* **1991**, *56*, 255. (c) Garcia-Garibay, M. A.; Zhang, Z.; Turro, N. J. *J. Am. Chem. Soc.* **1991**, *113*, 6212. (d) Turro, N. J.; Zhang, Z. *Tetrahedron Lett.* **1989**, *30*, 3761.

(5) (a) Steiner, U. E.; Wolff, H.-J. In *Photochemistry and Photophysics*; J. F. Rabek, J. F., Scott, G. W., Eds.; CRC Press: Boca Raton, FL, 1991; Vol. IV. (b) Steiner, U. E.; Ulrich, T. *Chem. Rev.* **1989**, *89*, 51. (c) Salikhov, K. M.; Molin, Y. N.; Sagdeev, R. Z.; Buchachenko, A. L. *Spin Polarization and Magnetic Effects in Radical Reactions*; Elsevier: Amsterdam, 1984.

(6) (a) Fendler, J. H.; Fendler, E. J. *Catalysis in Micellar and Macromolecular Systems*; Academic Press: New York, 1975. (b) Tanford, C. *J. Phys. Chem.* **1972**, *76*, 3020.

(7) (a) deKanter, F. J. J. Ph.D. Thesis, Tilburg, 1978. (b) Closs, G. L.; Doubleday, C. H., Jr. *J. Am. Chem. Soc.* **1973**, *95*, 2735. (c) Doubleday, C. H., Jr. *Chem. Phys. Lett.* **1979**, *64*, 67.

0002-7863/92/1514-9517$03.00/0

transfer from aniline to the thionine triplet in reversed micelles[8] shows an increase with a decrease in the size of the water pools. Similarly, the rate of geminate reaction of the RP comprised of phenoxyl and butyrophenone ketyl radicals in ionic sulfate micelles has been found to increase with a decrease in the micelle size.[9]

In contrast to these results, it has been found that an increase in the micelle size, achieved either by increasing the hydrocarbon chain length in the detergent molecule or by the addition of salts, results in an increase of the cage effect as measured by the yields of products obtained during photolysis of micellized 4-methyldibenzyl ketone.[10] A similar increase in the cage effect with an increase in micelle size, as measured by laser flash photolysis, was found for the photolysis of micellized alkyl phenyl ketones. In both instances it was the cage effect on the secondary radical pairs that was detected.[10]

The decrease in the cage effect as the micelle size decreases is consistent with the rate of exit of the radical fragments from the micelles increasing faster than the increase of the rate of reactive encounters; the net result is a diminution of the cage effect. This conclusion is in contradiction with a simple geometrical model for the cage effect. From purely spatial considerations, the rate constant of encounters (k_{enc}) of the radical fragments is proportional to L^{-3} (assuming that the viscosity of a spherical micellar core of radius L is invariant with the micellar size),[10,11] while the exit rate (k_{esc}) is at best proportional to L^{-2}.[12] Therefore, on the basis of simple geometrical arguments, the cage effect is expected to be proportional to $(k_{enc}/k_{esc}) \propto L^{-1}$. The conclusion is that there must exist factors other than geometric ones which allow for a faster increase in the value of k_{esc} relative to the rate of *reactive encounters*. These reasons may be chemical in nature, such as a chemical modification of the radical pair, or they may be physical in nature, such as a change in the probability of reaction per encounter due to a modulation of distance-dependent interactions.

To define in greater detail the mechanisms that operate on the micellized RP and affect their geminate reactivity, we have undertaken a quantitative investigation of the influence of the micellar size on the efficiency of the geminate reaction of two different RPs. These investigations have involved the use of different techniques including the magnetic isotope effect (MIE), ^{13}C-CIDNP, stimulated nuclear polarization (SNP), probability of geminate RP recombination, and the magnetic field effect on the efficiency of geminate chemical reaction (MARY).

In this first paper of a series, we present the results from the measurements of probability of recombination (P_r) of triplet geminate radical pairs (GRP). Two different radical pairs have been studied: (1) GRP_1, consisting of benzoyl/*sec*-phenethyl radicals, obtained from the photolysis of optically active methyldeoxybenzoin (MDB) and (2) GRP_2, consisting of acyl–*sec*-phenethyl/*sec*-phenethyl radicals, obtained from the photolysis of diastereomerically pure 2,4-diphenylpentan-3-one (DPP). The probabilities were determined by measuring the efficiency of isomerization as a function of conversion (the snip and knit approach[13]) in micelles of different sizes (L) at zero external magnetic field. Interestingly and importantly, these two pairs show contrasting behavior in their dependences of P_r on L. We suspected that the major difference between these two systems is the mode and rate of disappearance of the primary geminate RP. The GRP_1 from MDB is lost by chemical reactions (both spin selective and nonselective, such as reaction with detergent, oxygen, etc.) and diffusive escape through the micellar boundary; this rate for a very closely related benzoyl/cumyl RP is 5×10^6 s^{-1}.[14] The GRP_2 from DPP has in addition to these channels a rapid spin nonselective decarbonylation pathway[15] ($k_{-CO} = 4.9 \times 10^7$ s^{-1}) that is insensitive to the location of the acyl radical for the loss of the GRP. Besides this major difference, all other known parameters of molecular, spin, and chemical dynamics are almost the same.

An earlier model which considers escape of radicals from micelles to be a homogeneous process[3c,d,16] and gives excellent fitting of the magnetic field effects (MFE) on RP_1[3d] and SNP and CIDNP[3c] experiments for dibenzyl ketone (DBK) fails to rationalize our micelle size dependency results. We have carried out the necessary modifications to the model, and escape is now represented as a "spin nonselective chemical reaction" of the radicals with the boundary of the micelle[17] in the improved model. In particular, we show that this improvement and the distance-dependent ESE are the key determinants in explaining our experimental results.

Experimental Section

Gas chromatographic analyses were carried out using Hewlett-Packard 5890 gas chromatographs with flame ionization detectors on 25-m Carbowax 20M or 25-m SE-30 capillary columns and Hewlett-Packard 3390 or 3392 electronic integrators.

The meso and *d,l* forms of 2,4-diphenylpentan-3-one (DPP) were synthesized and purified according to known methods.[18] Optically active (*S*)-(+)-methyldeoxybenzoin (MDB) was prepared from optically active alanine (Aldrich Chemical Co.) as reported by McKenzie et al.[19]

Sodium dodecyl sulfate (SDS = C_{12}) was obtained from Bio-Rad and used as received. All other detergents were obtained from Lancaster Synthesis and purified by recrystallization from ethanol–ether mixtures. Ketone concentrations used were ~3.3 mM for MDB and ~3 mM for DPP. The concentrations of the detergents used were sodium dodecyl sulfate (C_{12}) = 100 mM, sodium undecyl sulfate (C_{11}) = 100 mM, sodium decyl sulfate (C_{10}) = 120 mM, sodium nonyl sulfate (C_9) = 130 mM, and sodium octyl sulfate (C_8) = 200 mM.

Photolyses, with the filtered light ($\lambda > 310$ nm) from a 1000-W high pressure Xe–Hg lamp, were performed on aqueous solutions of micelles which were thoroughly purged with argon prior to and during photolysis. After photolysis, the reaction solutions were extracted with a mixture of methylene chloride/ethyl acetate, a known amount of a GC standard (dibenzyl ketone, DBK) was added, and the mixture was dried over $MgSO_4$ and analyzed by capillary GC to measure conversion for MDB (SE-30) and DPP (Carbowax 20M) and isomer purity for DPP.

The optical purity of the MDB was measured by recording the circular dichroism spectrum, on a Jasco J-500 spectrometer, of photolysis solutions which had been diluted three times with stock SDS solution to obtain a suitable optical density. The presence of the detergents has no influence on the linearity of the intensity of CD spectrum of MDB with enantiomeric excess.

Experimental Results and Discussion

Photochemical Paradigm. Comparison of the UV spectra of DPP and MDB in hexane, methanol, and aqueous micellar solution indicates that both molecules are solubilized in the Stern layer of the micelle since both of them display a blue shift, relative to hexane, in the n,π^* band upon micellization. For the case of MDB, we find λ_{max} (ϵ) = 323 nm (165) in hexane, 321 (210) in ethanol, and 317 (252) in SDS solution.

Both MDB[20] and DPP[18] undergo homolytic α cleavage from a photoexcited state to generate GRP_1 and GRP_2, respectively. In micellar solutions these RPs effectively recombine to regenerate

(8) Ulrich, T.; Steiner, U. E. *Chem. Phys. Lett.* **1984**, *112*, 365.
(9) Evans, C. H.; Scaiano, J. C.; Ingold, K. U. *J. Am. Chem. Soc.* **1992**, *114*, 140.
(10) (a) Turro, N. J.; Zimmt, M. B.; Lei, X.-G.; Gould, I. R.; Wilemske, K. S.; Cha, Y. *J. Phys. Chem.* **1987**, *91*, 4544. (b) Turro, N. J.; Weed, G. C. *J. Am. Chem. Soc.* **1983**, *105*, 1861.
(11) (a) Gosele, V.; Klein, U. K. A.; Hauser, M. *Chem. Phys. Lett.* **1980**, *68*, 291. (b) Hatlee, M. D.; Kozak, J. J.; Rothenberger, G.; Infelta, P. D.; Gratzel, M. *J. Phys. Chem.* **1980**, *84*, 1508. (c) Tachiya, M. In *Kinetics of Nonhomogeneous Processes. A Practical Introduction for Chemists, Biologists, Physicists and Material Scientists*; Freeman, G. R., Ed.; John Wiley: New York, 1987; pp 575. (d) Gratzel, M.; Thomas, J. K. *J. Am. Chem. Soc.* **1973**, *95*, 6885.
(12) Almgren, M.; Greiser, F.; Thomas, J. K. *J. Am. Chem. Soc.* **1979**, *101*, 2021.
(13) Tarasov, V. F.; Ghatlia, N. D.; Buchachenko, A. L.; Turro, N. J. *J. Phys. Chem.* **1991**, *95*, 10220.
(14) Gould, I. R.; Zimmt, M. B.; Turro, N. J.; Baretz, B. H.; Lehr, G. P. *J. Am. Chem. Soc.* **1985**, *107*, 4607.
(15) (a) Turro, N. J.; Gould, I. R.; Baretz, B. H. *J. Phys. Chem.* **1983**, *87*, 531. (b) Lunazzi, L.; Ingold, K. U.; Scaiano, J. C. *J. Phys. Chem.* **1983**, *87*, 529.
(16) Tarasov, V. F.; Shkrob, I. L.; Step, E. N.; Buchachenko, A. L. *Chem. Phys.* **1989**, *135*, 391.
(17) Luders, K.; Salikhov, K. M. *Chem. Phys.* **1985**, *98*, 259.
(18) Baretz, B. H.; Turro, N. J. *J. Am. Chem. Soc.* **1983**, *105*, 1310.
(19) McKenzie, A.; Roger, R.; Wills, G. O. *J. Chem. Soc.* **1927**, 779.
(20) (a) Lewis, F. D.; Magyar, J. G. *J. Am. Chem. Soc.* **1973**, *95*, 5973. (b) Heine, H. G.; Hartman, W.; Kory, D. R.; Magyar, J. G.; Hoyle, C. E.; McVey, J. K.; Lewis, F. D. *J. Org. Chem.* **1974**, *39*, 691.

Scheme I. Possible Reaction Pathways for the Geminate Radical Pair from MDB

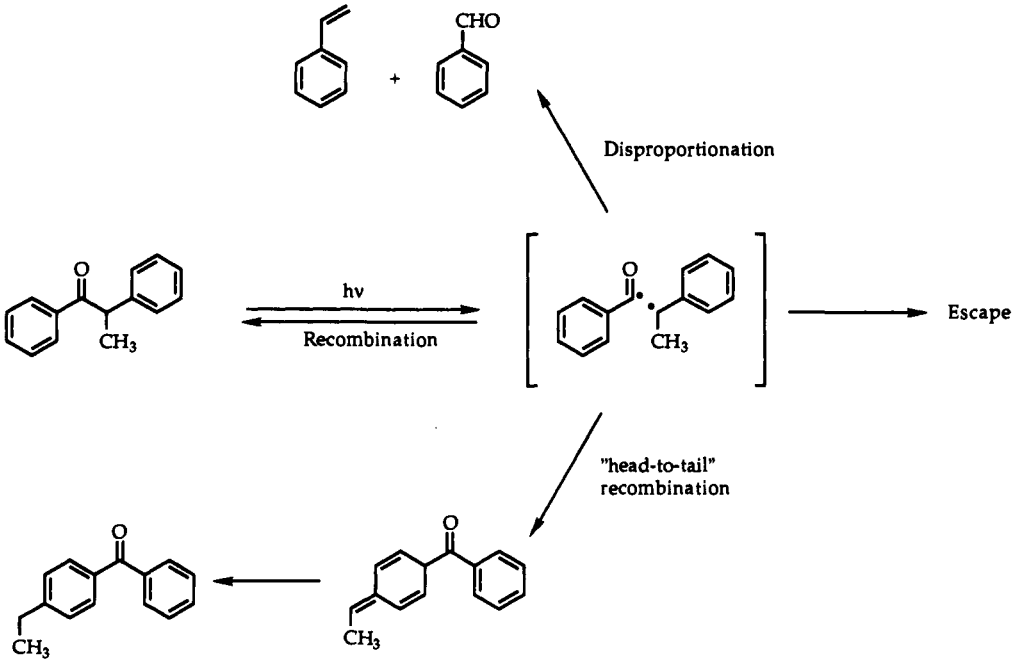

substrate ketone, isomerize (racemization for MDB and diastereomerization for DPP), disproportionate to produce styrene and the corresponding aldehyde, and escape into the bulk aqueous phase from the micelle (shown in Scheme I for MDB). The GRP_1 undergoes head-to-tail type coupling followed by a H atom rearrangement to generate ethylbenzophenone, while the GRP from DPP can undergo decarbonylation ($k_{-CO} = 4.9 \times 10^7\ s^{-1}$) to generate the secondary RP comprising of two *sec*-phenethyl radicals.

All processes associated with GRP_2 dissolved in SDS[13,18] are known to occur in the micellar phase. We will show later that this conclusion is also valid for the smaller micelles that we have investigated.

No such conclusion is immediately evident for the GRP_1, derived from MDB, since the benzoyl radicals do not decarbonylate. The observation of 2,3-diphenylbutane (DPB, chemical yield ~ 14% in SDS) suggests that *sec*-phenethyl radicals effectively recombine either in the aqueous phase or in the micelle phase due to the exchange between different micelles. That the *sec*-phenethyl radicals escape into water is supported by a sharp increase in the yield of 1-phenylethanol in the presence of $CuCl_2$ as an aqueous scavenger with hexadecyltrimethylammonium chloride (HDTCl) micelles (the yield of 1-phenylethanol in the absence of $CuCl_2$ is negligibly small). Product analysis fails to reveal even trace quantities of benzil, indicating that the recombination in the bulk aqueous phase of two benzoyl radicals that have escaped the micelle cage is a negligible process (since photolysis in homogeneous solution results in the formation of benzil in high yield[20b]). Therefore, we conclude that recombination processes to regenerate MDB outside the micellar phase are negligible. This conclusion is further bolstered by the observation that the efficiency of racemization of MDB in both SDS and HDTCl is unperturbed by the presence of $CuCl_2$, an efficient scanvenger of benzyl radicals.

Micelles. A simple conceptual geometrical picture of micellar structure leads to the prediction of a linear relationship between the number of carbon atoms in the longest alkyl chain of the detergent monomer unit (C_N) and micellar size (measured as some effective value).[6b] These values, as estimated by Tanford,[6b] are given in Table I. Note that several factors, including a nonspherical shape, detergent dynamics, a finite size distribution, the uncertainty in location, and diffusion of the radicals in the micellar core, all conspire to prevent a definition of an exact size for a micelle containing a dissolved organic substrate. Therefore, the values presented in Table I should be considered as effective or operational values which monotonically increase with an increase in the chain length of the detergent.

Table I. Physical Parameters Used for Different Alkyl Sulfate Micelles

micelle (C_N)[a]	10^8L, cm[b]	10^6D, $cm^2 \cdot s^{-1}$[c]
C_{12}	15.4	0.80
C_{11}	14.2	1.05
C_{10}	12.9	1.20
C_9	11.6	1.45
C_8	10.3	1.78

[a] N = the number of carbon atoms in the detergent molecule. [b] According to Tanford[6b] the maximum length l_{max} for a chain with n_c embedded carbon atoms, in Å, is $l_{max} = 1.5 + 1.265n_c$. Therefore, for C_{12}, $l_{max} = 16.68$. This value should be decreased by r (=3 Å) to compute the volume of the sphere that may be probed by a diffusing radical of radius r. However, since the radicals may also experience the Stern layer the effective radius should be increased by ~1.5 Å resulting in a net value of 15.4 Å for C_{12} micelles. We have used this value for C_{12} micelles and the Tanford increment for the other homologs to fit all the data presented in this paper. The same values of L have also been used to fit CIDNP magnetic field dependence, SNP, and magnetic isotope separation experiments which will be the subject of future publications. [c] We used a value of D in $C_{12} = 0.8 \times 10^{-6}$ $cm^2 \cdot s^{-1}$ based on the measured viscosity of SDS micelles as η = 8–12 cP.[22] The values of D for the other micelles were computed using the approximation that $D \times \tau_c$ = constant.

The other important micellar parameter relevant to this study is the viscosity (η) of the micellar phase. This parameter is critical since both the rate of encounters and the exit rate depend on it. Furthermore, the efficiency of the electron spin exchange (ESE) depends on the viscosity of the medium.[5] In order to determine the viscosity of the micellar aggregates, we have measured rotational correlation times (τ_c) of stable nitroxide radicals, using electron paramagnetic resonance spectroscopy, solubilized in the micelles of different sizes; these micelles are made using aqueous solutions of surfactants with varying chain lengths. The nitroxide probes include both 2,2,4,4-tetramethylpiperidinyl-*N*-oxyl (TEMPO) and a TEMPO-substituted benzophenone derivative

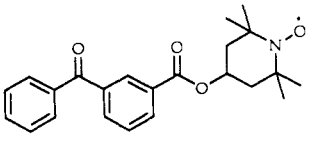

1

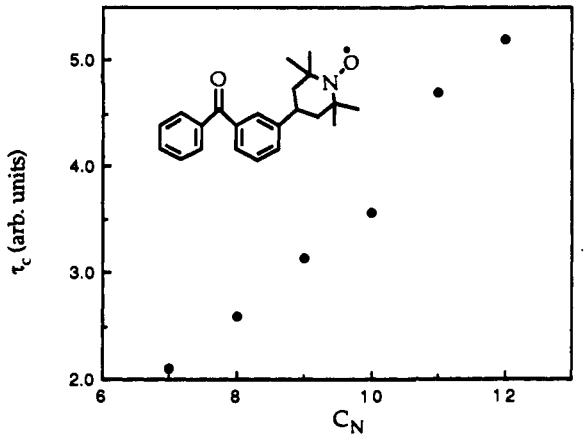

Figure 1. Dependence of rotational correlation times of **1** solubilized in alkyl sulfate micelles of different chain lengths C_N (N = number of carbon atoms in the detergent molecule).

(1). The results from these experiments are presented in Figure 1. It is evident that τ_c increases almost linearly with chain length.

Debye's formula relates rotational correlation times in direct proportionality with the viscosity of the medium. Thus, the viscosity of the micellar core for rotational motion increases approximately linearly with C_N. Other studies have shown that rotational and translational diffusion coefficients on alkyl sulfate micelles vary in a parallel fashion.[21] Stated differently, this means that the product of τ_c and D, where D is the diffusion coefficient of the radicals within the micelle, is invariant with micelle size. This relationship was applied to estimate the D values presented in Table I.

Experimental Methods. The two diastereomeric forms of DPP, *d,l*-DPP (racemic mixture) and *meso*-DPP (optically inactive), are readily distinguishable by chromatographic analysis. The kinetic analysis of this system[13] is based upon the fact that photoracemization in DPP cannot occur in one step and interconversion amongst the *d* and *l* forms must occur through the intermediacy of the meso diastereomer (Scheme II).

Methyldeoxybenzoin has only one asymmetric center. Free rotation of the GRP partners, generated from MDB, prior to recombination, results in photoracemization (Scheme II). The enantiomeric purity of the sample can be convieniently monitored using circular dichroism.[16,20a]

No significant photoisomerization (racemization for MDB and diastereomerization for DPP) for either of these systems is detected during photolysis in homogenous solution,[23] indicating that photoenolization or other mechanisms of isomerizations that do not involve bond cleavage may be neglected in any kinetic consideration.

Let x = [*meso*-DPP] or [(*S*)-(+)-MDB] and y = [*d,l*-DPP] or [(*R*)-(−)-MDB]. The time evolution of the isomeric concentrations, in light of the discussion above, in terms of the reaction probability approach may be described as[13,16]

$$\begin{aligned} dx/dt &= -W_x[x(1 - P_{xx})] + W_y y P_{yx} \\ dy/dt &= -W_y[y(1 - P_{yy})] + W_x x P_{xy} \end{aligned} \quad (1)$$

where W_x and W_y are the specific rates of RP formation from x and y isomers, respectively. P_{ik} is the probability of geminate recombination in which the subscripts i and k imply a corresponding configuration of the precursor and product, respectively.

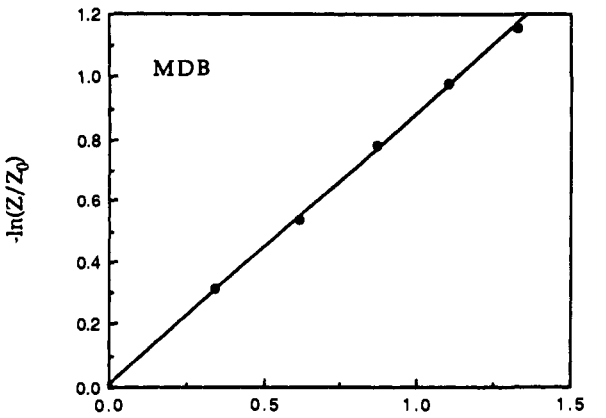

Figure 2. Racemization of MDB as a function of conversion in C_{10} micelles.

Scheme II. Photoisomerization in MDB and DPP

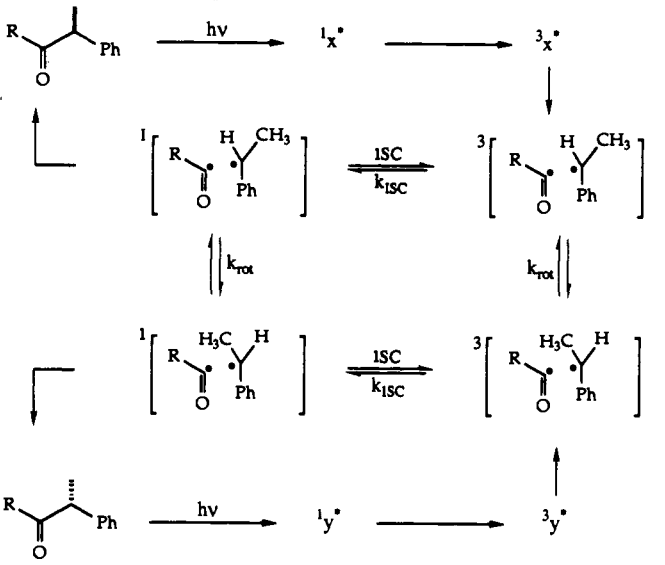

R = Ph for MDB

= $PhCH(CH_3)$ for DPP

One may solve eq 1 (for the case of DPP only in an approximate form[13]) to obtain

$$\log (Z/Z_0) = S[\log (1 - f)] \quad (2)$$

with

$$S = 2P_{inv}/(1 - P_{inv} - P_{ret}) = 2P_{inv}/(1 - P_r) \quad (3)$$

where $P_{inv} = P_{xy} = P_{yx}$ is the probability of recombination with inversion of configuration, $P_{ret} = P_{xx} = P_{yy}$ is the probability of recombination with retention of configuration, $P_r = (P_{inv} + P_{ret})$ is the total recombination probability, $Z = (x - y)/(x + y)$ is the isomeric purity (Z = enantiomeric excess for MDB and Z = diastereomeric excess for DPP), and f is the total ketone conversion at the point of measurement of Z.

For the case of MDB, $P_{inv} = P_{ret}$ and

$$S = P_r/(1 - P_r) \quad (4)$$

For the case of DPP we have

$$S = [P_r/(1 - P_r)][1 \pm \Delta] \quad (5)$$

where Δ is the correction that is introduced to account for either a small difference in the quantum yield of dissociation for the *meso*-DPP and *d,l*-DPP isomers or for the existence of some

(21) Ottaviani, M. F. O.; Ghatlia, N. D.; Turro, N. J. *J. Phys. Chem.* **1992**, *96*, 6075.

(22) (a) Emert, J.; Behrens, C.; Goldenbery, H. *J. Am. Chem. Soc.* **1979**, *101*, 771. (b) Turro, N. J.; Aikawa, N.; Yekta, A. *J. Am. Chem. Soc.* **1979**, *101*, 772.

(23) Step, E. N.; Buchachenko, A. L.; Turro, N. J. Submitted for publication in *J. Org. Chem.*

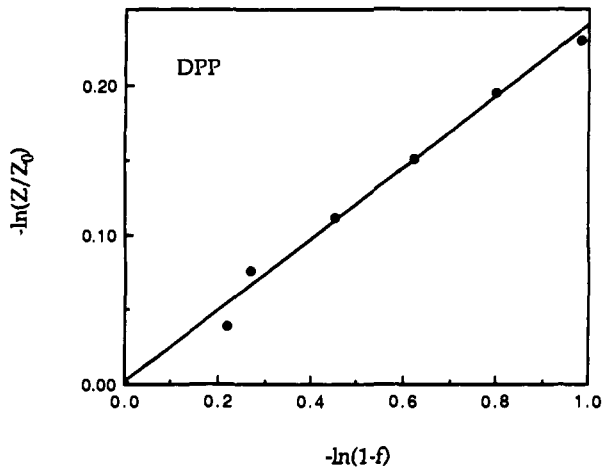

Figure 3. Diastereomerization of DPP as a function of conversion in C_{10} micelles.

Table II. Reaction Parameters for Radical Pairs Derived from MDB(GRP_1) and DPP(GRP_2)

	probability of recombination		estimated rates for GRP_1	
micelle	GRP_1	GRP_2	$k_z/4^a$	k_r^b
C_{12}	0.534 ± 0.011	0.165 ± 0.007	2.45×10^7	7.42×10^6
C_{11}	0.492 ± 0.008	0.180 ± 0.009	4.55×10^7	8.19×10^6
C_{10}	0.466 ± 0.012	0.201 ± 0.011	8.02×10^7	8.23×10^6
C_9	0.422 ± 0.017	0.227 ± 0.008	1.62×10^8	7.44×10^6
C_8	0.335 ± 0.013	0.228 ± 0.012	3.75×10^8	5.78×10^6

[a] See eq 9. [b] The values of k_r were estimated from the calculation of P_r under the assumption of a constant value of $k_e = 5 \times 10^6$ s^{-1} independent of micelle size, bf = 0, $J_0 = 13 \times 10^9$ rad·s^{-1}, $\lambda = 5 \times 10^{-9}$ cm. See Table I for values of L and D. $k_r = Pk_e/(1 - P)$.

stereoselectivity in the GRP recombination.

Examples of the excellent applicability of eqs, 2–5 are shown in Figures 2 and 3. Equations 4 and 5 were used to measure P_r for DPP and MDB in different micelles. The dependence of the recombination probability, in zero magnetic field, on the number of carbon atoms in the individual detergent molecules is depicted in Figure 4. The quantitative data are presented in Table II, from which it follows that the recombination probability P_r *decreases* with decreasing C_N for GRP_1 but *increases* with decreasing C_N for GRP_2.

The problem that needs to be considered is *how do we rationalize the qualitatively and quantitatively different dependences of the geminate recombination probability upon the micelle size*?

Time Intervals for Radical Pair Recombination in the Micelle Phase. It is fruitful to consider the radical pair dynamics in the micelle in terms of three different physical processes and the time scales associated with them. Since these three processes occur simultaneously, there is no chronology to the associated time scales.

The first time interval corresponds to usual geminate reencounter of a radical pair and can be estimated as[5c]

$$\tau_G = R^2/D \tag{6}$$

where D is the coefficient of mutual diffusion of two particles, assuming that they are diffusing in a nonrestricted space whose viscosity is equal to the microviscosity of the core, and $R = r_1 + r_2$ where r_1 and r_2 are the radii of the radical fragments.

$$D = D_1 + D_2 = \frac{k_B T}{6\pi\eta}\left[\frac{1}{r_1} + \frac{1}{r_2}\right] \tag{7}$$

Using the values of D presented in Table I and approximating $R = 6$ Å ($r_1 = r_2 = 3$ Å), we find that τ_G varies from 4.5×10^{-9} to 2×10^{-9} s in C_{12} through C_8 micelles, respectively.

The second time interval marks the end of the period where geminate recombination may be thought of as occuring in an unrestricted volume. It is the time required for the first visit to the boundary of the micelle. For a rough approximation we use[11d,17]

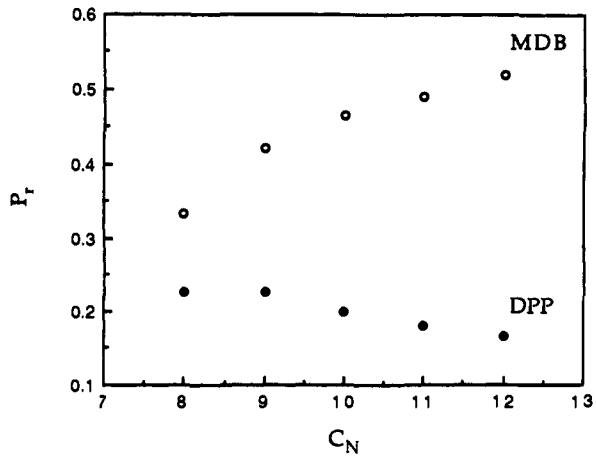

Figure 4. Dependence of geminate recombination probability of GRP_1 from MDB (○) and GRP_2 from DPP (●) as a function of C_N.

$$\tau_1 = L^2/D \tag{8}$$

where L is the radius of the sphere within whose volume the radical is free to diffuse. The value of τ_1 ranges from 3×10^{-8} s for C_{12} to 6×10^{-9} s for C_8 micelles.

Radicals are not assured of escape from the micelle phase upon the first visit to the boundary since there is a potential barrier[12,24] preventing this process. This leads to reencounters. The rate of this reencounter process, forced by the micellar boundary, can be defined by the constant k_z, in the long time approximation,[11b,c] as

$$k_z = \lambda_1^2 D \tag{9}$$

where λ_1 is the first positive root of the equation

$$\lambda_1 L = \tan[\lambda_1(L - R)]$$

Thus, k_z ranges from 1×10^8 s^{-1} for C_{12} to 1.5×10^9 s^{-1} for C_8 micelles. The time interval $\tau_z = k_z^{-1}$ can be called the time of "filling out". After this time, the decay of the radicals is close to monoexponential.[11] Comparison of τ_z with τ_1 shows that the first is shorter than the second. We recognize this to be a reflection of the approximations used since, from a physical perspective, τ_1 should be less than τ_z.

Both GRP_1 and GRP_2 are unsuitable for investigation by nanosecond flash photolysis: the absorption spectrum of the excited triplet state of MDB interferes with the detection of the benzylic radicals in GRP_1, while rapid decarbonylation ($\tau \sim 22$ ns[15]) restricts the lifetime of GRP_2. We have therefore used time-resolved SNP to measure the decay rate constant in GRP_1. Preliminary results[25] show that the observed decay rate constant changes from 7×10^6 s^{-1} for C_{12} to 8.6×10^6 s^{-1} for C_8 micelles. Thus, most of the RP decays after the filling out time. This is true even in the case of GRP_2, since the estimations of the filling out time ($\sim 10^{-8}$ s) are smaller than the time of decarbonylation ($\sim 2.2 \times 10^{-8}$ s) even for SDS, the largest micelle studied. This sluggishness of geminate reaction relative to all the transient time periods described above allows us to use a simple kinetic treatment wherein all processes may be considered to be first order.

Two obvious possibilites may explain the sluggishness of the GRP decay: (1) reaction in the singlet state is extremely ineffective or (2) there exist processes which retard the intersystem crossing (ISC) in the RPs or decrease the percentage of singlet character.

Prediction of the Kinetic Treatment. To a crude approximation,[26] the ISC process may be divided into two separate parts:

(24) Almgren, M.; Greiser, F.; Thomas, J. K. *J. Am. Chem. Soc.* **1979**, *101*, 2021.
(25) Avdievich, N.; Bagrayanskaya, I. A.; Tarasov, V. F. Unpublished results.
(26) (a) Tarasov, V. F.; Shkrob, I. A. *Khim. Physica* **1990**, *9*, 812. (b) Shkrob, I. A.; Tarasov, V. F. *Chem. Phys.* **1990**, *147*, 369.

Scheme III. Generalized Kinetic Scheme for Micellized Primary Geminate Radical Pair

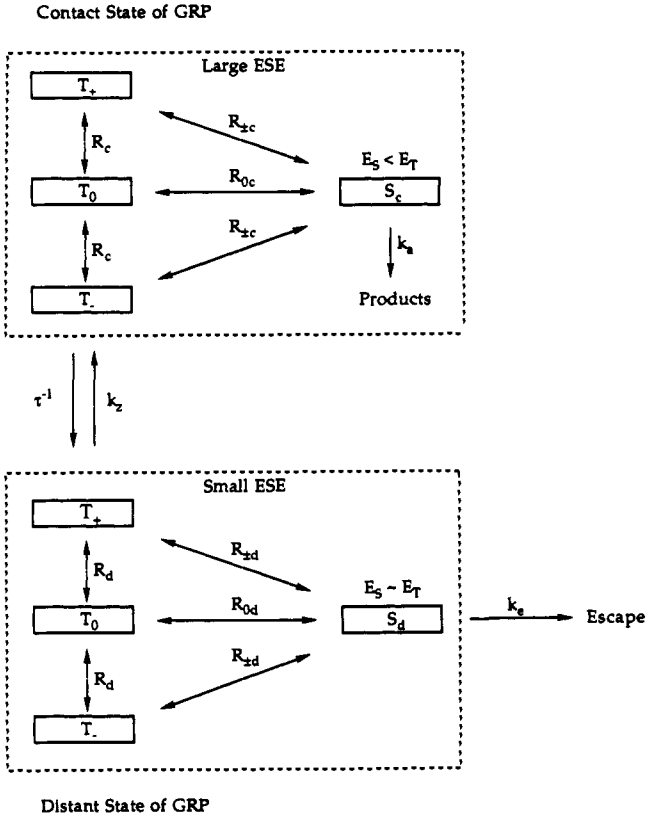

(1) ISC in radical pairs separated by a short distance (contact RPs which we denote as RP_c) and (2) ISC in radical pairs separated by a long distance (distant radical paris which we denote as RP_d). The phenomenological delineation between distant and contact is that only RP_c can react to form a bond, while RP_d, even in the singlet state, cannot.

Let k_a be the rate constant for reaction of singlet RP_c, and let τ^{-1} be the rate constant that describes the process of separation of RP_c to form RP_d. τ here is defined as $\tau = \Delta R/D$ (Scheme III). Δ is the thickness of the spherical shell within which reaction may occur. Thus, a singlet radical pair whose centers are separated by a distance greater than $R + \Delta$ are physically prevented from reacting to form a bond.

For the contact RPs, the rate constant for the $T_0 \leftrightarrow T_\pm$ transition R_c should be large due to the existence of strong dipole–dipole interactions. Note that this assumption is not critical and is made only to simplify further mathematical analysis. The rate constants $R_{\pm c}$ and R_{0c}, arising due to hyperfine interactions (HFI), should be suppressed due to the exchange interaction in the RP_c. No difference between R_{0d} and $R_{\pm d}$ is assumed to exist in the distant RPs in zero magnetic field. Then, in the diffusion limit of chemical reactions and the conditions that $k_a \gg \max\{\text{all rate constants}\}$ and $R_c \gg \tau^{-1}$ (this condition means that an equilibration of $T_\pm$ and T_0 sublevel population due to dipole–dipole interaction has been achieved), we can solve the problem in the form

$$S = S_d + S_r \tag{10}$$

where S was defined in eq 4 with the substitution of P_r for a total reaction probability P.

The first term is given by

$$S_d = \frac{k_z \tau^{-1} l_d}{(k_z + \tau^{-1} + k_e) k_e (4l_d + k_z + k_e)} \tag{11}$$

and for the contact RPs we can write

$$S_c = \frac{l_c}{k_e} \frac{k_e + k_z}{(k_e + \tau^{-1} + k_z)} \tag{12}$$

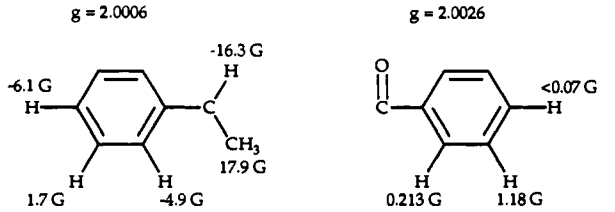

Figure 5. Magnetic parameters used for the RPs. Only the HFI with the CH_3 and CH protons in the *sec*-phenethyl radical are taken into account in the theoretical calculations with a distance-dependent ESE.

where $3l_{d,c} = 2R_{\pm d,c} + R_{0d,c}$.

Let us now suppose that ISC in RP_d is governed primarily by HFI. Then the value of l_d estimated from quasiclassical approximations[3e,5,27,28] is 1.7×10^8 s^{-1} (see Figure 5 for the HFI constants[29]).

The dependence of k_e on the micellar size may be estimated as follows. Let us suppose that the boundary of the micelle absorbs radicals in a very narrow layer of thickness $\Delta' \ll L$ with the rate constant $k_{out} \ll k_a$. Then $\Delta' k_{out} L/D \ll 1$; the implication of the last inequality is that the probability of "reaction" of the radicals with the boundary per encounter is small. A simple consideration of the corresponding diffusional problem leads to the formula for the observed rate constant as

$$k_e = 3\Delta' k_{out}/L \tag{13}$$

We assume that the value for k_e for GRP_1 in C_{12} equals the experimentally measured value for the closely related radical pair of benzoyl/cumyl radicals; $k_e = 5 \times 10^6$ s^{-1}.[14] Using this value we can predict the values of k_e in other micelles with the aid of eq 13 and the assumption that the product $\Delta' k_{out}$ is invariant with micelle size.

Then for GRP_1 the calculations, according to eq 11, predict an increase in S_d with decreasing L from 3.03 for C_{12} to 12.4 for C_8. The contribution of S_c to S can not be large since $l_d \gg l_c$ (due to ESE suppresed S–T interconversion in the contact state) and $\tau(4l_d + k_z + k_e) \ll 1$. Furthermore, S_c increases with decreasing L also. An increase in S translates to an increase in P with a decrease in micelle size. *This prediction, obtained under the approximation that only HFI defines the ISC, is in stark contrast with the experimental data.*

For the case of DPP, we have $k_e(\text{DPP}) = k_{-CO} + k_e(\text{MDB})$. All other parameters are considered to be the same. Corresponding calculations predict an increase in S_d for DPP from 0.35 in C_{12} to 1.60 in C_8 micelles. In this instance the qualitative prediction of an increase in P with a decrease in L is borne out by the experimental results. However, the experimental value of S does not rise as sharply as that predicted by this treatment.

Accurate Model. According to the kinetic scheme presented above, the value of S (and hence of P) can vary in direct proportion to L either provided that l_d (a measure of the ISC rate) $< (k_z + k_e)/4$ or that l_d is a function of micelle size and decreases as L decreases. Intuitively it is clear that a decrease in the micelle size should lead to an increase in some effective or operating ESE, leading to a consequent reduction in the rate of ISC. However, it is not obvious that the increase in the effective ESE is sufficient to decrease the cage effect in GRP_1 (despite the fact that the rate of encounters increases as L^{-3} at least!) with a decrease in micelle size but is not strong enough to prevent an increase in the cage effect in GRP_2. The motivation behind our computer modeling is to try and determine whether such conditions in which l_d is dependent on the micelle size can actually be realized.

Our theoretical consideration of the problem is based on two main concepts: (1) the model of the microreactor[11,30] and (2) the

(27) Nakagaki, R.; Hiramatsu, M.; Watanabe, T.; Tanimoto, Y.; Nagakura, S. *J. Phys. Chem.* **1985**, *89*, 3222.
(28) Weller, A.; Nolting, F.; Staerk, H. *Chem. Phys. Lett.* **1983**, *96*, 24.
(29) *Landbolt-Bornstein: Organic C Centered Radicals*; Fisher, H., Hellwege, K.-H., Eds.; Springer–Verlag: Berlin, 1977; Vol. 1, Part b.
(30) (a) Tarasov, V. F.; Maltsev, V. I.; Buchachenko, A. L.; *Russ. J. Phys. Chem.* **1981**, *55*, 1921. (b) Sterna, L.; Ronis, D.; Wolfe, S.; Pines, A. *J. Phys. Chem.* **1980**, *73*, 5493.

Pederson–Freed differential scheme[31] to solve the Liouville equation. The model is considered in detail in the supplementary material provided. It is important to stress that in contrast to an earlier method,[3c,d] where the escape rate of the GRPs was considered as a monoexponential process that is *independent of the location of the radicals in the micelles*, the accurate model uses a micelle with a permeable boundary described by the parameter bf (see eq S2 in the supplementary material), which we call the "boundary factor"

$$\mathrm{bf} = \frac{k_{\mathrm{out}}\Delta' L}{D} \tag{14}$$

Thus, the observed rate constant of escape can be described as follows:

$$k_e = 3\mathrm{bf}D/L^2 \tag{15}$$

Since D/L^2 can be interpreted as the rate constant of the encounters of the radicals with the boundary (see eq 8), bf may be interpreted as the probability for the radicals to be "absorbed" by the boundary per unit encounter. The appearance of the factor 3 in eq 15 is a consequence of the crudity of the estimation of the rate constant of the first visit to the boundary defined by eq 8. The condition bf = 0 implicates a perfectly reflecting micellar boundary.

We are far from the goal that allows us to physically model the penetration of the radical through the boundary. Furthermore, it is obvious that eq 14 is only a rough approximation, since the radicals can reenter the micelle after crossing the boundary; however, this process is disallowed under the model. An attempt to model this process leads to inordinate increases in the computation time and was therefore discarded. We also assume that the dimensionless parameter bf is independent of micelle size.

ESE is the only distance-dependent interaction considered by us, and we shall demonstrate that this is enough to model the experimental results. Theoretical modeling of ISC rate constants in the frame of such an approximation has been done by Bittl and co-workers,[32] but they were forced to make additional assumptions, especially for zero and small magnetic fields. Modeling the probabilities of recombination can be done in a far more rigorous form, but much information regarding rates of processes is sacrificed in such an effort. Therefore, additional efforts to check the results from a kinetic viewpoint are warranted.

The ESE exchange is modeled to be exponential in nature

$$J(r) = J_0 \exp[-(r - R)/\lambda] \tag{16}$$

where J_0 is the orientationally averaged value for the exchange potential in the RP at $r = R$. A typical value for λ is 5×10^{-9} cm.[32] Values for J_0 will be discussed later.

Limitations on the Application of the Model. In the frame of this model, one can consider HFI with only a limited number of nuclei in the radical fragments—we consider only four protons with the largest HFI constants (see Figure 5). This results in a noticeable decrease,[16,33] in zero magnetic field, of the calculated probability of reaction relative to the experimental value. For the case of GRP_1, to compare the experimental and theoretical values of P_r we must multiply the theoretical value by a factor of 0.7. This is done to account for the fact that 30% of the GRP which reacted yielded products other than starting ketone or the enantiomer (yield of the disproportionation product benzaldehyde was ~20%, and yield of the head-to-tail coupling product ethylbenzophenone, for low conversions, was ~10%), while the experimentally determined P_r measures only recombination. The theoretical values resulting from this multiplication are noticeably smaller, by factors of 0.75–0.85, than the experimental values. Since the qualitative agreement between the functional behavior of the theoretical and experimental values is sufficient, we have used a scaling factor to overcome this shortcoming of our model. These values for the scaling factors lie in the range of 1.05–1.15 for both GRP_1 and GRP_2.

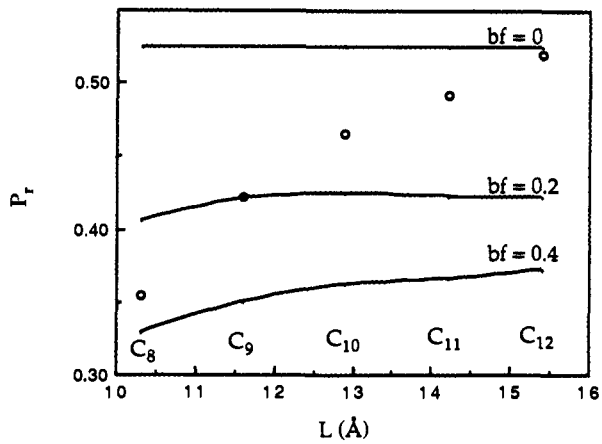

Figure 6. Calculated dependence of P_r upon L for GRP_1 under the assumption of a negligibly small ESE with different boundary factors: $D = D(L)$; $k_s\tau = 10$ and $k_e = 1 \times 10^5$ s^{-1} (to model the slow spin nonselective reactions). The experimental points are presented as O.

Another obvious shortcoming of our model is the absence of any ISC due to paramagnetic relaxation. Prohibitively long computation times preclude any attempt to include these processes along with those of multinuclear HFI and a distance-dependent ESE. In earlier work we found that quantitative fitting of experimentally measured P_r values in C_{12} micelles for GRP_1 can be achieved with the supposition that GRP_1 is born in a state with equilibrated singlet and triplet spin level (25% singlet character for the initial RP) populations.[16] This may be considered as a crude approximation of possible fast paramagnetic relaxation. However, the possibility of partial dissociation from the singlet state[34] cannot be ignored. Note that this approximation is not needed for the short-lived GRP_2.

Results of Calculations and Discussion

Four particular characteristics of the system are relevant to the discussion: (1) the micelle size, (2) the permeability of the micelle boundary, (3) the distance dependence of the exchange interaction, and (4) the dependence of the viscosity of the micellar core on C_N.

Exchange Interaction. Figure 6 presents results from the calculated values of P_r for GRP_1 under the conditions that $J \sim 0$ (a value of 5×10^6 rad·s^{-1} was used to facilitate the computation process) and that D is a function of micelle size ($D = D(L)$, see Table I) and for three different values of bf = 0.0, 0.2, and 0.4 This figure clearly demonstrates that it is *impossible to mimic the experimental trend in P_r, even qualitatively, under the approximation of negligible ESE.*

Figure 7a and 7b give the dependence of P_r upon J_0 for different micelle sizes for GRP_1 and GRP_2, respectively. These calculations were performed under the condition that $D = D(L)$ and bf = 0.08 for all the micelles. For MDB, $k_e = 1 \times 10^5$ s^{-1} (for modeling slow spin nonselective reactions), and for DPP, $k_e = 4.9 \times 10^7$ s^{-1} (rate of decarbonylation). Figure 7a shows that there is only a weak dependence of the calculated values of P_r on J_0 for values of $J_0 > 5 \times 10^9$ rad·s^{-1}. This allows us only to estimate a lower bound on the value of J_0 for the case of MDB. In the case of DPP (Figure 7b), the values of J_0 must be smaller than 3×10^8 rad·s^{-1} to accurately mimic the experimental dependence of P_r on L. The final values used were $J_0 = 13 \times 10^9$ rad·s^{-1} for GRP_1 and $J_0 = 2.5 \times 10^9$ rad·s^{-1} for GRP_2. These values also provide excellent fits when modeling the results of additional experiments which will be the subjects of future publications.

The value of J_0 for GRP_2, derived from DPP, is noticeably smaller than that for RP_1, derived from MDB. It should be

(31) (a) Pedersen, J. B.; Freed, J. H. *J. Chem. Phys.* **1974**, *61*, 1517. (b) Zientara, G. P.; Freed, J. H. *J. Chem. Phys.* **1979**, *70*, 1359.
(32) Bittl, R.; Schulten, K.; Turro, N. J. *J. Chem. Phys.* **1990**, *93*, 8260.
(33) Salikhov, K. M. *Chem. Phys.* **1983**, *82*, 163.
(34) Sakata, T.; Takahashi, S.; Terazima, M.; Azumi, T. *J. Phys. Chem.* **1991**, *95*, 8671.

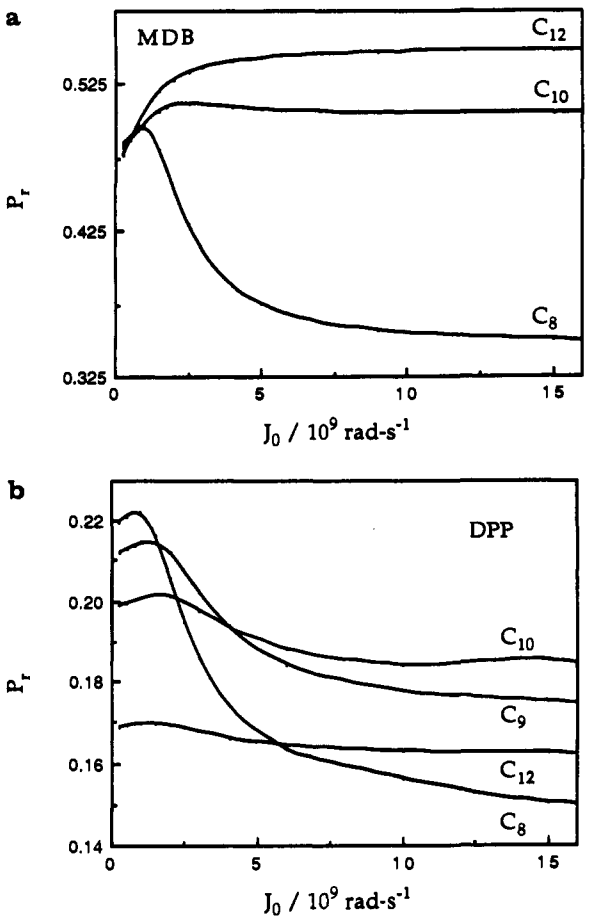

Figure 7. Calculated dependence of P_r upon J_0 (a) for GRP_1 and (b) for GRP_2. In both cases $D = D(L)$, bf = 0.08, $k_s\tau = 10$, and HFI constants are from Figure 5. $k_e = 1 \times 10^5$ s^{-1} for RP_1, and $k_e = 4.9 \times 10^7$ s^{-1} for RP_2.

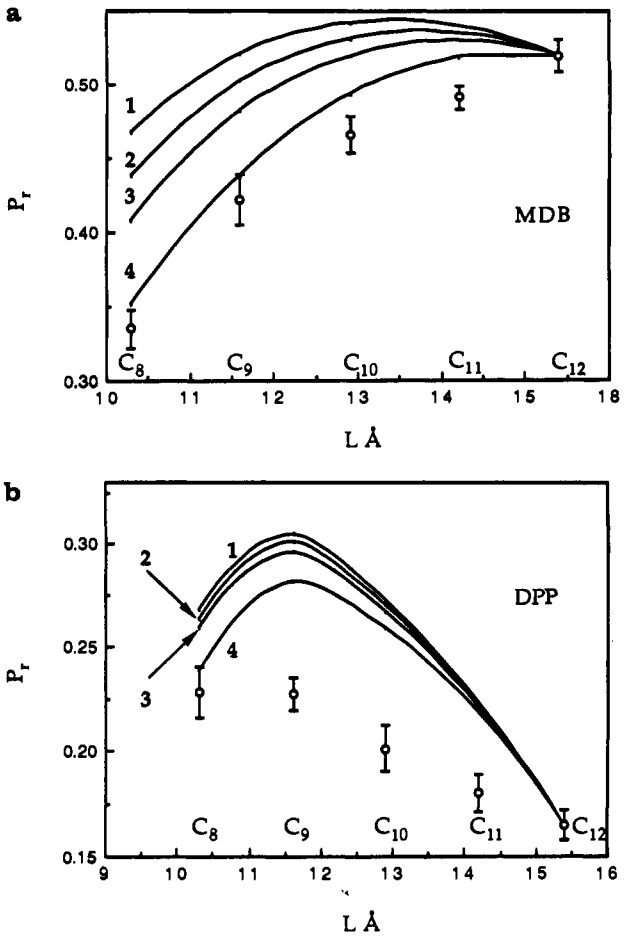

Figure 8. Calculated dependence of P_r on L for (a) GRP_1 derived from MDB and (b) GRP_2 derived from DPP. Both cases reflect the condition that bf = 0 (perfectly reflecting boundary). Curve 1 is for the condition of k_e = constant; curve 2 results when $k_e \propto 1/L$; curve 3 arises when $k_e \propto 1/L^2$; and curve 4 summarizes the situation for $k_e \propto 1/L^4$. For GRP_1, k_e(MDB) in $C_{12} = 5 \times 10^6$ s^{-1}, $J_0 = 13 \times 10^9$ rad·s^{-1}, and $D = D(L)$. For GRP_2 k_e(DPP) = k_e(MDB) + 4.9×10^7 s^{-1}, $J_0 = 2.5 \times 10^9$ rad·s^{01}, and $D = D(L)$. The experimental values are presented as O.

emphasized here that the magnitude of J_0 is defined by the geometrical averaging of ESE interactions between the spin centers. In the limit of fast reorientation[3c]

$$|J_0| \sim k_B T(f_a f_b) \sim k_B T[\lambda^2/4r_1r_2]^2 \qquad (17)$$

where one assumes that ESE in the contact of spin centers is of the order of k_BT and f_i are geometrical factors.

According to eq 17, a 5-fold decrease of J_0 implies that the radius of the acyl-*sec*-phenethyl radical is ~2 times larger than the radius of the benzoyl radical. This seems to be an unrealistic figure; however, we should note that the presence of the extra methyl group on the acyl radical from DPP will increase the average separation between the partners of the RP_c from DPP relative to the RP_c from MDB. This will result in a further decrease in J_0.

Permeability of Micelles. Figures 8a and 8b give the results from a calculation of P_r for MDB and DPP, respectively, under the assumption of a perfectly reflecting boundary (bf = 0) and $D = D(L)$. Four curves are presented in each figure, and they are computed with the additional conditions listed below. For curve 1, the value of the homogeneous k_e is independent of micelle size and takes the value 5×10^6 s^{-1} for RP_1 and 5.4×10^7 s^{-1} for RP_2 since k_e(DPP) = k_{-CO} + k_e(MDB). Curve 2 is calculated under the assumption that $k_e \propto L^{-1}$. Curve 3 is calculated for $k_e \propto L^{-2.12}$ which is equivalent to the assumption that bf does not depend on the micelle size (see eq 15). Curve 4 is calculated for $k_e \propto L^{-4}$. These calculations were performed under the conditions of a distance-dependent ESE since Figure 6 clearly shows that in the approximation of negligible ESE not even a qualitative match between theory and experiment is found. Note that $k_e \propto L^{-4}$ gives a reasonable fit for GRP_1 (curve 4 in Figure 8a). However, the escape rate in this condition, especially in the small micelles, becomes very fast and essentially exceeds even the decay rate constants measured by the time-resolved SNP technique. For the C_8 micelle the value of k_e in this approximation is 2.5×10^7 s^{-1}, whereas the measured decay rate constant is 8.6×10^6 s^{-1}.[25] These calculations for a perfectly reflecting boundary and homogeneous first-order escape process give results that are very similar to those obtained from the kinetic treatment. The general characteristic for both approaches is the physically impossible proposition that radicals from MDB escape homogeneously from any point within the micelle. Therefore, *all attempts to model escape as a homogeneous first-order process were unfruitful.*

Viscosity Effect. The dependence of P_r upon L, when one neglects the dependence of D on the micelle size is presented in Figure 9 for MDB. Curves for two different values of $D = 2 \times 10^{-6}$ cm^2·s^{-1} and $D = 1 \times 10^{-6}$ cm^2·s^{-1} are shown. From these curves it is seen that the value of D must change by approximately a factor of 2 upon going from C_{12} to C_8 micelles. A 2-fold change in D values is in agreement with the measured values of τ_c and the corresponding calculated values of D (see Figure 1 and Table I).

Thus, the computer simulations unequivocally demonstrate that the dependence of P_r does not follow the trend predicted by geometric factors alone; only by invoking ESE into consideration can a qualitative and quantitative reproduction of the experimental data be achieved. However, the geometrical properties, including the bf and the dependence of D on L, are not insignificant, and *omission of any one of these considerations also leads to the disappearance of even qualitative similarities.* The excellent fits

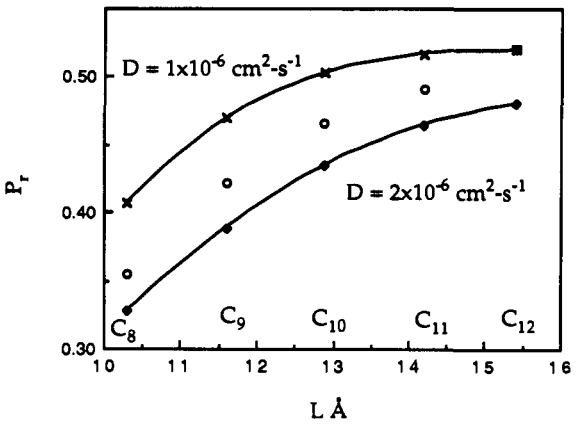

Figure 9. Calculated dependence of P_r upon L and comparison with experimental results (O) for GRP_1 from MDB. The parameters used were $J_0 = 13 \times 10^9$ rad·s^{-1}, bf = 0.08, $k_e = 1 \times 10^5$ s^{-1}, and $D = 1 \times 10^{-6}$ cm^2·s^{-1} (upper curve) and $D = 2 \times 10^{-6}$ cm^2·s^{-1} (lower curve).

that we have obtained by a simultaneous consideration of all these parameters can be seen as the solid lines in Figures 10a and 10b.

Qualitative Considerations. To qualitatively understand the disparate behavior of GRP_1 and GRP_2 in terms of their dependences of P_r upon L, we consider the simplest case of a radical pair, born in the triplet state and posssesing only one magnetic nucleus, in the field of some constant effective exchange interaction J_{eff}. In this case the probability of finding the GRP in the singlet state may be derived analytically as

$$|c_s(t)|^2 = \frac{3a^2}{G} \sin^2 \{(G)^{1/2}t\} \tag{18}$$

where

$$G = 4a^2 - 2J_{effa} + J_{eff}^2 \tag{19}$$

$a = A/4$ (the situation when the triplet state is higher in energy than the singlet state corresponds to $J > 0$ in the formula for G), J_{eff} is the effective exchange interaction, and A is the HFI.

The characteristic time for geminate reaction is 10^{-7} s, while the characteristic values $G^{1/2}$ exceed 10^9 rad·s^{-1}. Therefore, we can average the $|cs(t)|^2$ value for the purposes of qualitative considerations. This means that the reaction rate constant can be expressed as

$$k_r \propto (3a^2/2G)k_z \tag{20}$$

where k_z is the rate constant of encounters. From eq 20 it is clear that k_r does not vary monotonically with J_{eff} if $J_{eff}A < 0$ but rather has an extremum in the range of $J_{eff} \sim A/4$. This property carries over to multinuclear systems with a distance-dependent ESE, too. In our cases, the conditions $J_{eff}A < 0$ is actually satisfied since $J_0 < 0$ and positive HIF predominate.

To determine an approximate functional form for J_{eff} in terms of the micelle size, we artificially divide the distance between the radicals into two parts. The first one corresponds to small values of ESE where HFI-induced ISC is allowed, and the second corresponds to close distances where ESE suppreses ISC. The boundary point between these two divisions can be defined[31b] as occuring at r^* by $J(r^*) = \sigma A$, where σ is a coefficient of proportionality which may be determined by simulation of the experimental results or by comparison with an exact solution. We now consider ESE only in the range of $L > r > r^*$, since ISC in the range of $r < r^*$ is suppressed and the contribution of this range to the total reaction probability can be expressed through the simple target parameter R/r^*. Since the behavior of ESE in the range of $r > r^*$ is independent of J_0 $\{J(r) = \sigma A \exp[-(r - r^*)/\lambda]\}$, we see that J_{eff} is a function of A, r^*, L, λ, and possibly D and k_e(bf) $\{J_{eff} = f(r^*,\lambda,\sigma A,L,D,k_e)\}$. In reality, J_{eff} is implicitly dependent on J_0 but only through a very weak logarithmic dependence of r^* on J_0:

$$r^* = R + \lambda \ln (J_0/\sigma A) \tag{21}$$

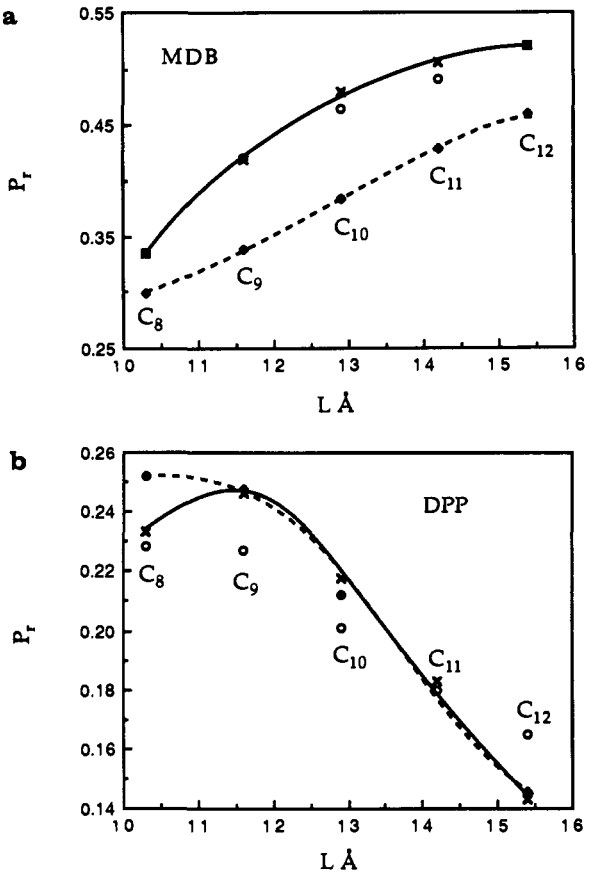

Figure 10. Comparison of experimental (O) and computational results (solid line is for distance-dependent ESE and dashed line is calculated according to J_{eff} determined by eq 22) for (a) GRP_1 from MDB, $J_0 = 13 \times 10^9$ rad·s^{-1}, $k_e = 1 \times 10^5$ s^{-1} and (b) for GRP_2 from DPP, $J_0 = 2.5 \times 10^9$ rad·s^{-1}; $k_e = 4.9 \times 10^7$ s^{-1}. All other parameters are the same for both the RPs: HFI constants are from Figure 5, $\lambda = 5 \times 10^{-9}$ cm, $R = 6 \times 10^{-8}$ cm, $D = D(L)$; $k_s\tau = 10$, and bf = 0.08.

This is in excellent agreement with the results of accurate calculations, depicted in Figure 7, from which it can be seen that P is independent of J for large values of J_0 for all micelle sizes, while the value of P for a fixed micelle size increases only when J_{eff} decreases.

In particular, for the case of fast encounters, when averaging of ESE along the diffusional trajectories occurs, it is possible to find J_{eff}. In this approach we have

$$J_{eff} = 3\sigma A\lambda r^{*2}/L^3 \tag{22}$$

The greater sensitivity of P_r to J_0 in small micelles is a consequence of the fact that in these situations r^* is now comparable in value of L, and an increase in r^* relative to L causes a sharp decrease in the range where ISC due to HFI is effective. Note also that extremely large values of J_0 lead to the situation where $r^* > L$, and then the approximations fail again.

Figures 10a and 10b present the calculated values of the reaction probability as a function of micelle size in the frame of the model of an effective exchange interaction (dotted lines) according to eq 22. It is clear from these figures that this model is effective in describing the experimental situation when the value of σ parameter is chosen to be ~ 5.

Estimations of Rate Constants. The computer experiments show (Figure 10) that a reasonable reproduction of the experimental data is achieved when we consider a distance-dependent ESE, $D = D(L)$ and bf = 0.08–0.04. From a kinetic standpoint, the value of bf is slightly high since it leads to estimated escape rate constants (eqs 14 and 15) $k_e = (9.6–4.8) \times 10^6$ s^{-1}. However, it should not be forgotten that eq 15 is crude and that the model neglects the reentry of the radical back into the micelle phase. Allowing for reentry will lead to a decrease in k_e relative to irreversible escape

and bring it closer to the experimentally measured value of the exit rate constant.

From the calculated probabilities of the geminate reaction P, one may estimate the reaction rate constant according to the relation $P = k_r/(k_r + k_e)$, where k_r is the rate of reactive encounters. The results from such an estimation are presented in the fourth column of Table II. A comparison of these values with the estimated values for the rate constant of all encounters dramatically demonstrates the profound influence of ESE on the reaction rate constants. Only in C_{12} micelles is k_r comparable with $k_z/4$, while in C_8 micelles it is almost 100 times smaller. The values of k_r themselves have only a very weak dependence on micelle size, and this is in agreement with the experimental determinations using laser flash photolysis[14] or time-resolved SNP[25] experiments and with the prediction of eq 20.

Conclusions and Remarks

Based on the observation of monoexponential decay, Scaiano[35] introduced a very simple kinetic scheme summarized by the equation below

$$P_r = k_r/(k_r + k_e) \text{ or } S = k_r/k_e$$

This scheme has been widely utilized in the interpretation of data from laser flash experiments.[5,14,36] However, a difficult problem arises with the physical interpretation of k_r—the rate constant of reaction. A common interpretation is that k_r is the rate of ISC and consequently that ISC is the rate-limiting step for the recombination reaction. From a different perspective, experimental results measuring the magnetic field dependence of k_r[14] or P_r[16] are in agreement with the hyperfine mechanism as are the estimations of the isotope separation efficiencies.[26] But this estimation that the rate-determining step $k_r = k_{ISC}$ is in contradiction with the estimation of k_{ISC} from the hyperfine mechanism, which yields $k_{ISC} = 2 \times 10^8$ s^{-1} for the system under consideration where $k_{ISC} \gg k_r$.

To resolve this dilemma we introduced another kinetic scheme[26] whose salient feature was the separation of the RPs into contact and distant RPs. The phenomenological interpretation, according to this model, is that k_r is the rate constant of GRP encounters in the micellar phase; k_r and not k_{ISC} was the rate-determining step in that consideration. In our early work we estimated k_r in this approximation and found good agreement with experimental results. However, our estimations[26] were based on the value for the mutual diffusion coefficient of 3×10^{-7} cm^2·s^{-1} and a micelle size for SDS of $L \sim 20$ Å. We now believe that the diffusion coefficient used was smaller and that the micelle size used was larger than the correct value. It should, however, be pointed out again that the selection of these parameters is an ambiguous and complex process. We believe that the parameters employed in this study are reasonable and that they lead to the prediction that the value of $k_z/4$ is larger than k_r.

The model which considers only HFI mechanism for ISC leads to the incorrect prediction, for MDB, that the recombination probability should decrease when the micelle size increases. Of the parameters tested, only the introduction of ESE, which retards the rate of ISC, allows one to quantitatively fit the experimentally measured probabilities of recombination. The implication of this for the Scaiano scheme is that k_r is not purely the rate of encounters, as per our earlier estimations, but is closer to the ISC rate in the RP. We now believe that ISC is the rate-limiting step in these reactions, especially in small micelles; the interactions responsible for this ISC are not purely HFI but rather are HFI attentuated by ESE. The decrease in the micelle size leads to an increase of the effective ESE and an increase in the escape rate of the radicals. These two effects combine to lead to a retardation of the rate of ISC and a decrease in the cage effect in the case of MDB as the size of the micelle decreases. For DPP, however, this ESE-induced retardation of the rate of ISC is not effective enough to lead to a decrease in the cage effect with a decrease in micelle size. This is especially valid since the effective rate constant of escape is essentially the same in all the micelles, resulting in a domination of the effect of an increase of the rate of encounters.

Computer modeling clearly demonstrates that there is no need to invoke any other distance-dependent interactions besides ESE ($J_0 > 5 \times 10^9$ rad·s^{-1} for MDB and $J_0 < 3 \times 10^9$ rad·s^{-1} for DPP) to explain the experimental observations. This explanation also requires a micelle size-dependent diffusion coefficient (ranging from $D \sim 0.8 \times 10^{-6}$ cm^2·s^{-1} for C_{12} to 1.8×10^{-6} cm^2·s^{-1} for C_8) and the introduction of a penetrable micelle boundary.

Preliminary considerations suggest that the solution to the problem of escape rate may be obtained by direct measurement of the k_e and its dependence on the micelle size; yet it should not be forgotten that (i) the measurement of the escape rate is strongly dependent on the kinetic scheme used and (ii) the reentry of the radicals into the micellar phase should be taken into accout. The last process and its influence on the quantitative results have not been considered yet.

A qualitative solution of this problem results in the conclusion that the influence of a distance-dependent ESE on the rate of geminate RP reaction in a micellar cage can be taken into account by the introduction of a "spin factor" (see eq 20) in addition to the usual steric factor as a crude approximation.

Thus this paper has attempted to demonstrate that for geminate radical pair reactions in micelles the important interconnection between characteristic sizes and reaction times originates due to distance-dependent interactions. The effect of these interactions is experimentally manifest, despite the fact that they are extremely weak from the point of view of usual considerations of overlap of electronic functions and are far from the values which are energetically comparable with k_BT.

Acknowledgment. The authors at Columbia would like to thank the Air Force Office of Scientific Research, the National Science Foundation, and the Department of Energy for generous support of this research. The authors at Moscow would like to thank Max Barkov for fruitful discussions and the ICP Co. for financial support. We would also like to thank Dr. Miguel A. Garcia-Garibay for kindly providing us with a sample of **1**.

Supplementary Material Available: Further information on some of the terms and equations used in this paper (3 pages). Ordering information is given on any current masthead page.

(35) Scaiano, J. C.; Abuin, E. B.; Stewart, L. C. *J. Am. Chem. Soc.* **1982**, *104*, 5673.

(36) Levin, P. P.; Kuzmin, V. A. *Izv. Akad. Nauk SSSR, Ser. Khim.* **1988**, 1873.